Nonlinear Dynamics **38:** 117–131, 2004.

Numerical Simulations of Fractional Systems: An Overview of Existing Methods and Improvements

MOHAMED AOUN[1,*], RACHID MALTI[2], FRANÇOIS LEVRON[3], and ALAIN OUSTALOUP[1]
[1]*LAP – UMR 5131 CNRS – Université Bordeaux I – ENSEIRB, 351 Cours de la Libération, 33405 Talence cedex, France;* [2]*IS – UT de Sénart – Université Paris 12, Avenue Pierre Point, 77127 Lieusaint, France;* [3]*Institut de Mathématique de Bordeaux, Université de Bordeaux I, 351 Cours de la Libération, 33405 Talence cedex, France;* **Author for correspondence (e-mail: aoun@lap.u-bordeaux1.fr; fax: +33-540-006644)*

(Received: 28 April 2003; accepted: 16 March 2004)

Abstract. An overview of the main simulation methods of fractional systems is presented. Based on Oustaloup's recursive poles and zeros approximation of a fractional integrator in a frequency band, some improvements are proposed. They take into account boundary effects around outer frequency limits and simplify the synthesis of a rational approximation by eliminating arbitrarily chosen parameters.

Key words: continuous time model, discrete time model, fractional model, fractional calculus, modeling, numerical simulation

1. Introduction

The concept of differentiation to an arbitrary order (fractional differentiation) was defined in the 19th century by Riemann and Liouville. Their main concern was to extend differentiation by using not only integer but also non-integer orders. In the field of system identification studies on real systems, such as electrochemical [1, 2] or thermal [3, 4], reveal inherent fractional differentiation behavior. The use of classical models, based on integer order differentiation, is thus inappropriate in representing these fractional systems. Thus, a further class called fractional models has been developed since 1945 [5–7] using the concept of fractional differentiation.

A major difficulty with fractional models is time-domain simulation. Often, the analytical solution of a model's output is not simple to compute. During the last 20 years numerical algorithms have been developed using either continuous or discrete rational models approximating fractional systems [7–12]. Some of their advantages, disadvantages, and improvements are presented in Section 3. Finally some numerical examples are given. But, first the basic definitions of fractional calculus are outlined.

2. Fractional Linear Models: Mathematical Background

The fractional integral of a function $f(t)$ is defined by [16]:

$$\left(I_{t_0}^{n} f\right)(t) \triangleq \frac{1}{\Gamma(n)} \int_{t_0}^{t} \frac{f(\tau)}{(t-\tau)^{1-n}} d\tau, \tag{1}$$

where $t > t_0$ and n is the real positive integration order. $\Gamma(n)$ is the Euler Gamma function:

$$\Gamma(n) = \int_0^\infty \mathrm{e}^{-x} x^{n-1} dx. \tag{2}$$

The Laplace transform of the integral of $f(t)$ is given by:

$$\mathcal{L}\{I_0^n f(t)\} = \frac{1}{s^n} F(s), \tag{3}$$

where $F(s)$ is the Laplace transform of $f(t)$.

The Riemann–Liouville fractional derivative of non-negative order n of $f(x)$ is defined as [17]:

$$D_{t_0}^n f(t) \triangleq \left(\frac{d}{dt}\right)^m \left(I_{t_0}^{m-n} f(t)\right), t > t_0, \tag{4}$$

where m is the smallest integer greater or equal to n.

Second definition is given by Grünwald:

$$D_{t_0}^n f(t) = \lim_{h \to 0} \frac{1}{h^n} \sum_{j=0}^{(t-t_0)/h} (-1)^j \binom{n}{j} f(t - jh), (t - t_0) \text{ is a multiple of } h \tag{5}$$

where

$$\binom{n}{j} = \frac{\Gamma(n+1)}{\Gamma(j+1)\Gamma(n-j+1)}$$

Definitions (4) and (5) are equivalent when $f(t_0) = D_{t_0}^1 f(t_0) = \cdots = D_{t_0}^\infty f(t_0) = 0$.

Fractional integration and fractional differentiation of order $n = 0$ of a function reproduces the function to which it is applied.

From Equation (5), note that fractional differentiation is not a local operator, because Newton's binomial is not zero when $j > n$ and $n \notin \mathbf{N}$, whereas it is zero when $j > n$ and $n \in \mathbf{N}$. Hence, $D_{t_0}^n f(t_1)$ depends on the whole past of $f(t)$, $t \in [t_0, t_1]$, unless differentiation order n is integer where it reduces to local past values. For example when $n = 1$:

$$D_0^1 f(t) = \lim_{h \to 0} \frac{f(t) - f(t-h)}{h}. \tag{6}$$

When $f(0) = D_0^1 f(0) = \cdots = D_0^\infty f(0) = 0$ the Laplace transform of $D_0^n f(t)$ [18] is:

$$\mathcal{L}\{D_0^n f(t)\} = s^n F(s). \tag{7}$$

This result is coherent with the classical case when n is an integer. Consequently, it is easy to define a symbolic representation of a dynamic system, such as a transfer function.

Based on the definitions above, a Single Input Single Output (SISO) Linear Time Invariant (LTI) system H, relaxed at $t = 0$ are described by a differential equation:

$$D^{n_{a_1}} y(t) + a_2 D^{n_{a_2}} y(t) + \cdots + a_L D^{n_{a_L}} y(t) = b_1 D^{n_{b_1}} u(t) + \cdots + b_J D^{n_{b_J}} u(t) + e(t), \tag{8}$$

where $a_2, \ldots, a_L, b_1, \ldots, b_J$ are real and $u(t)$, $y(t)$, $e(t)$ are respectively input, output and noise signals. All differentiation orders $n_{a_1}, \ldots, n_{a_L}$ and $n_{b_1}, \ldots, n_{b_J}$ are allowed to be fractional (integer or non integer).

As H is relaxed, the Laplace transform of $D^{n_a} y(t)$ and $D^{n_b} u(t)$ are respectively $s^{n_a} Y(s)$ and $s^{n_b} U(s)$ where $Y(s)$ and $U(s)$ are the Laplace transforms of $y(t)$ and $u(t)$.

Applying the Laplace transform to Equation (8) yields:

$$s^{n_{a_1}} Y(s) + \cdots + a_L s^{n_{a_L}} Y(s) = b_1 s^{n_{b_1}} U(s) + \cdots + b_J s^{n_{b_J}} U(s) + E(s) \tag{9}$$

from which the generalized transfer function is deduced:

$$H(s) = \frac{Y(s)}{U(s)} = \frac{b_1 s^{n_{b_1}} + \cdots + b_J s^{n_{b_J}}}{s^{n_{a_1}} + \cdots + a_L s^{n_{a_L}}} = \frac{B(s)}{A(s)} \tag{10}$$

Any proper model ($n_{a_L} < \cdots < n_{a2} < n_{a1} > n_{b1} > n_{b2} > \cdots > n_{bJ}$) $H(s)$ can be represented by using a modal form, provided commensurate order condition is satisfied (all differentiation orders n_{a_1}, ..., n_{a_L} and $n_{b_1}, \ldots, n_{b_J}$ are multiples of a some same number, let it be n):

$$H(s) = \sum_{l=1}^{L} \frac{A_l}{(s^n - \lambda_l)^{q_l}} \tag{11}$$

where $l = 1, \ldots, L$, q_l is the multiplicity of the eigenvalue λ_l and n a real number known as commensurate differentiation order.

To simulate a fractional system it is useful to know if it is stable or not. Matignon has established the stability condition of any commensurate explicit fractional model having real differentiation orders [16, 21]. A commensurate (of order n) fractional system is stable if:

- $0 < n < 2$
- and for every $\lambda_l \in \mathbf{C}$, such that $A(s^n) = 0$ ($A(s^n)$ is the denominator of (10)):

$$|Arg(\lambda_l)| > n\frac{\pi}{2} \tag{12}$$

This allows the angle $n\frac{\pi}{2}$ to vary in $]0, 2\pi[$ (see Figure 1). The bigger n is, the smaller the stability region. When n tends to 2, the stability region tends to the half-line $\mathcal{R}^-$, and when $n \geq 2$ it vanishes. In the latter case, the modal representation of any transfer function $F(s)$ contains only unstable terms whatever λ_l are. The only integer inside]0,2[is [1]. Hence, for the classical rational systems, the only commensurate order which ensures stability is $n = 1$ and provided the Routh–Hurwitz stability criterion (12) ($n = 1$).

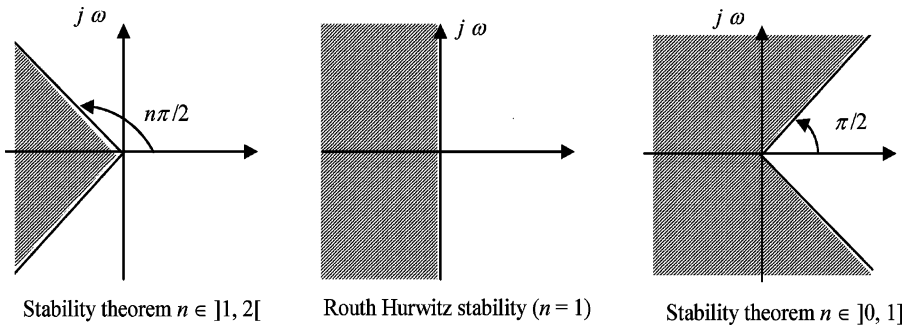

Figure 1. Stability region (shaded) for fractional commensurate systems.

3. Numerical Simulations

Simulation of fractional systems is complicated due to their long memory behavior as shown by Oustaloup [20]. Many methods have been developed during the last decade [7–12]. They can be classified into three groups:

- Methods based on the computation of analytical expression of the output.
- Methods based on the approximation of a fractional model by a rational discrete-time one.
- Methods based on the approximation of a fractional model by a rational continuous-time one.

3.1. Methods Based on an Analytical Expression of Output

The output of the system is computed using the modal form:

$$H(s) = \sum_{l=1}^{L} \frac{A_l}{(s^n - \lambda_l)^{q_l}}, \quad l = 1, \ldots, L. \tag{13}$$

Thus, the output of the system is a linear combination of eigenmode outputs. The *l*th output expression is given by:

$$y_l(t) = L^{-1}\left\{\frac{1}{(s^n - \lambda_l)^{q_l}}\right\} \otimes u(t) = h_l(t) \otimes u(t) \tag{14}$$

where $\otimes$ denotes convolution product and $h_l(t)$ is the Mellin–Fourier inverse Laplace-transform of $\frac{1}{s^n - \lambda_l}$.

In the particular case where $\lambda_l = 0$ and nq_l is not integer, $h_l(t)$ is:

$$h_l(t) = \mathcal{L}^{-1}\left(\frac{1}{(s^n)^{q_l}}\right) = \frac{1}{\Gamma(nq_l + 1)} t^{nq_l} \tag{15}$$

In the general case $h_l(t)$ is:

$$\begin{aligned} h_l(t) = \mathcal{L}^{-1}\left(\frac{1}{s^n - \lambda_l}\right)^{q_i} &= \sum_{k=1}^{\text{numberofpoles}} \frac{p_k}{\lambda_l^{q_i}} Q_{q_i - 1}\left(\frac{1}{n}, tp_k\right) e^{tp_k} \\ &+ \frac{1}{\pi} \int_0^{\infty} \frac{e^{-tx} \sum_{k=0}^{q_i - 1} (-1)^k \binom{q_i}{k} (\lambda_l)^k x^{n(q_i - k)} \sin[n\pi(q_i - k)]}{\left[x^{2n} - 2\lambda_l x^n \cos(n\pi) + \lambda_l^2\right]^{q_i}} dx, \end{aligned} \tag{16}$$

Q is a polynomial defined by:

$$\begin{cases} Q_0(x, y) = x \\ \kappa Q_\kappa(x, y) = (xy + x - y) Q_{\kappa - 1}(x, y) + xy \dfrac{\partial}{\partial y} Q_{\kappa - 1}(x, y) \end{cases}$$

When the eigenmode is not multiple ($q_1 = 1$), the expression of $h_l(t)$ is:

$$h_l(t) = \mathcal{L}^{-1}\left(\frac{1}{s^n - \lambda_l}\right) = \sum_{k=1}^{\text{numberofpoles}} \frac{s_k}{n\lambda_l} e^{ts_k} + \frac{\sin(n\pi)}{\pi} \int_0^{\infty} \frac{x^n e^{-tx}}{x^{2n} - 2\lambda_l x^n \cos(n\pi) + \lambda_l^2} dx \tag{17}$$

The first part of (16) and (17), called *exponential mode*, results from the computation of residue(s) on each pole of $\frac{1}{s^n-\lambda_l}$. The second part, called *aperiodic multimode* characterizes each fractional system and stems from an integral along the negative real axis of the Bromwich–Wagner contour [20].

In most cases the analytical expression of the output is not easy to obtain. In a simulation context, it requires the computation of the integral at every sampling period. Moreover, it depends on the precision used when computing the convolution integral in (14).

3.2. Methods Based on Discrete-Time Models

These methods approximate a fractional model by a rational discrete-time model. The fractional differentiator is substituted by its discrete-time equivalent. As a result a discrete-time transfer function is obtained:

$$H(z) = \frac{b_1(w(z^{-1}))^{n_{b_1}} + \cdots + b_J(w(z^{-1}))^{n_{b_J}}}{(w(z^{-1}))^{n_{a_1}} + \cdots + a_L(w(z^{-1}))^{n_{a_L}}}$$

$w(z^{-1})$ the discrete mapping of the Laplace operator s, can be computed using various approximation methods. The most common are Euler's, Tustin's, Simpson's, or Al-Alaoui's approximations [8, 9, 22]. These analogue-to-digital open-loop design methods lead to irrational z-transforms which are then approximated either by a truncated Taylor's series expansion or a continuous fraction expansion. The obtained digital model can then be simulated using a classical implementation structure: direct-form, parallel-form, cascade-form, lattice-form, etc.

It is important to point out that, whatever be the discrete approximation, the resulting model is a finite impulse response (FIR). Truncating the model corresponds to truncating time domain data. This is not in agreement with principle of infinite memory of fractional derivatives. Hence, the main drawback of these methods is that the order of the discrete-time model (see Table 1) depends on the sampling period and the length of the input signal. The order of the discrete-time model is at least equal to the data length. This makes real-time simulation hard to achieve.

It would be interesting to compare these different simulation methods numerically, to determine which performs better and in which context. Our aim is to present improvements to methods based on continuous time rational models.

Table 1. Discrete-time approximations of *sn*.

Euler (Grünwald)	Tustin
$s \to w(z^{-1}) = \frac{1}{T}(1 - z^{-1})$	$s \to w(z^{-1}) = \frac{2}{T}\frac{1 - z^{-1}}{1 + z^{-1}}$
$(w(z^{-1}))^n = \frac{1}{T^n}\left(1 - nz^{-1} + \frac{n(n-1)}{2}z^{-2} + \cdots\right)$	$(w(z^{-1}))^n = \left(\frac{2}{T}\right)^n (1 - 2nz^{-1} + 2 * n^2 z^{-2} + \cdots)$
Simpson	Al-alaoui
$s \to w(z^{-1}) = \frac{3}{T}\frac{(1 - z^{-1})(1 + z^{-1})}{1 + 4z^{-1} + z^{-2}}$	$s \to w(z^{-1}) = \frac{8}{7T}\frac{1 - z^{-1}}{1 + z^{-1}/7}$
$(w(z^{-1}))^n = \left(\frac{3}{T}\right)^n (1 - 4nz^{-1} + 2n(4n+3)z^{-2} + \cdots)$	$(w(z^{-1}))^n = \left(\frac{8}{7T}\right)^n \left(1 - \frac{8}{7}nz^{-1} + \left(-\frac{24}{49}n + \frac{32}{49}n^2\right)z^{-2} + \cdots\right)$

3.3. Methods Based on Continuous-Time Rational Models

In these methods the fractional model output is computed using an equivalent continuous-time rational model deduced from approximating a fractional integration operator by a rational one. Fractional behavior of a given system is usually limited in a frequency range. However, this is not a problem as long as input and output data are sampled prior to processing, which limits, *de facto*, the upper frequency band (due to the sampling period); the lower frequency band is limited by the input data spectrum. As a result, a fractional model and its rational approximation must have the same dynamics within a limited frequency range. The rational equivalent model is computed in three steps:

1. fractional integration behavior is represented by a fractional model in a limited frequency range;
2. the obtained fractional model is then approximated by a continuous-time rational model;
3. the model's output is then computed by discretizing the rational model as in the classical case.

Step 1 – Representing a fractional integration behavior using a fractional model in a limited frequency range

In the general case, the fractional behavior is localized in a limited frequency range which can be deduced from a rough analysis of system's behavior, input spectrum, and sampling period.

Let s^{-n} be a fractional integrator of order n, $0 < n < 1$, and $s^{-n}_{[\omega_\mathrm{A},\omega_\mathrm{B}]}$ a fractional model of s^{-n} in the desired frequency range $[\omega_\mathrm{A}, \omega_\mathrm{B}]$.

$$s^{-n}_{[\omega_\mathrm{A},\omega_\mathrm{B}]} \cong \frac{1}{s^n} \tag{18}$$

Oustaloup approximates the fractional integrator (18) in [7] by:

$$s^{-n}_{[\omega_\mathrm{A},\omega_\mathrm{B}]} = C_{(n)} \left(\frac{1 + (s/\omega_\mathrm{h})}{1 + (s/\omega_\mathrm{b})} \right)^n \tag{19}$$

Model (19) has null asymptotic behaviors at low and high frequencies. Hence, in some cases, there is a static error between the fractional model and its rational approximation. To set the static error to zero, Lin prefers using an approximation whose asymptotic behaviors correspond to a first-order integrator in low and high frequencies [23]:

$$s^{-n}_{[\omega_\mathrm{A},\omega_\mathrm{B}]} = \frac{C_{(n-1)}}{s} \left(\frac{1 + (s/\omega_\mathrm{h})}{1 + (s/\omega_\mathrm{b})} \right)^{n-1} \tag{20}$$

As the objective is to achieve a satisfactory approximation of the fractional behavior in the interval $[\omega_A, \omega_B]$, the approximation must be carried out over a larger interval namely $[\omega_b, \omega_h]$ in order to take into account boundary effects around frequencies ω_A and ω_B. In both approximations (19) and (20) ω_h and ω_b are chosen by a rule of thumb. Usually, they are set to $\omega_\mathrm{b} = \sigma^{-1}\omega_\mathrm{A}$ and $\omega_\mathrm{h} = \sigma\omega_\mathrm{B}$, where σ is adjusted arbitrarily around$\sqrt{10}$. The choice of σ depends mainly on differentiation order n and $[\omega_A, \omega_B]$. The static gain $C_{(.)}$ depends directly on differentiation order n, upper frequencies ω_h and frequencies lower ω_b:

$$C_{(n)} = \left| \left(\frac{1 + j\sqrt{\dfrac{\omega_\mathrm{b}}{\omega_\mathrm{h}}}}{1 + j\sqrt{\dfrac{\omega_\mathrm{h}}{\omega_\mathrm{b}}}} \right)^n \right|^{-1} \tag{21}$$

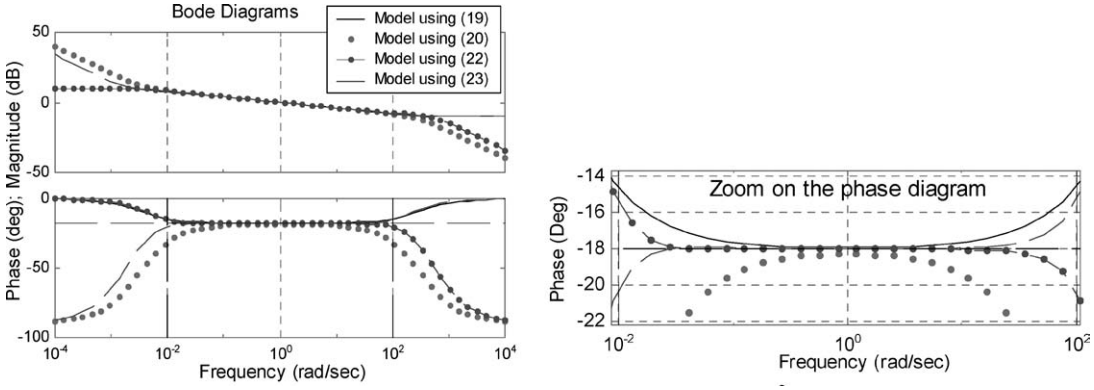

Figure 2. Fractional integration at order 0.2 approximated within $[10^{-2}, 100]$ with the same number of poles for all models.

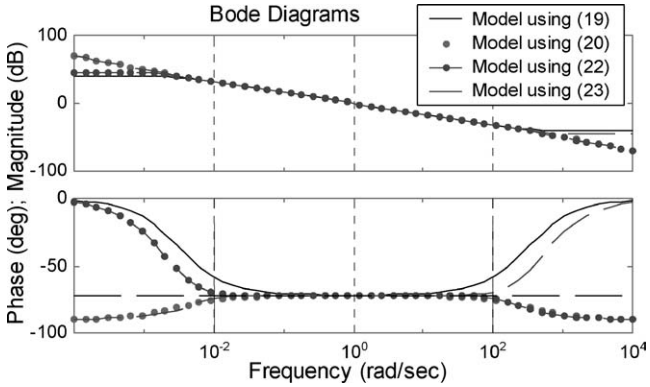

Figure 3. Fractional integration at order 0.8 approximated within [0.01, 100] with the same number of poles for all models.

A zoom on the phase diagram of a fractional integral of order n near zero, shows that the approximation error using (19) is less than with (20) (see Figure 2). However, when order n approaches 1, the error on the phase using approximation (19) becomes greater than the error using (20) (see Figure 3).

Two new approximations of s^{-n} are now proposed. Both are less sensitive to differentiation orders and need no arbitrary adjustment coefficients (such as ω_b and ω_h). Approximations are carried out directly by using the frequency range $[\omega_A, \omega_B]$ in which the fractional behavior is modeled. In both approximations, the static gain $C_{(n)}$ is replaced by a second order model which is computed in a particular manner.

Approximation (22) has an asymptotic behavior of a simple gain in low frequencies and a first-order integrator in high frequencies. It uses a second-order transfer function for $C_{(n)}$ with two poles and one zero.

$$s^{-n}_{[\omega_A,\omega_B]} \cong \frac{\omega_B(\omega_A + s)}{(\omega_A)^n(ns^2 + \omega_B s + (1-n)\omega_A\omega_B)} \left(\frac{1 + \dfrac{s}{\omega_B}}{1 + \dfrac{s}{\omega_A}} \right)^n \tag{22}$$

Approximation (23) has an asymptotic behavior of a first-order integrator in low frequencies and a simple gain in high frequencies. It uses a second-order transfer function for $C_{(n)}$ with two poles and

two zeros;

$$s^{-n}_{[\omega_A,\omega_B]} \cong \frac{\omega_A^{1-n}}{s}\left(\frac{(1-n)s^2+\omega_B s+n\omega_A\omega_B}{\omega_A\omega_B+s\omega_B}\right)\left(\frac{1+\dfrac{s}{\omega_B}}{1+\dfrac{s}{\omega_A}}\right)^{n-1} \tag{23}$$

Both approximations are synthesized (see the appendix) to minimize the difference between s^{-n} and $(\frac{1+\frac{s}{\omega_B}}{1+\frac{s}{\omega_A}})^n$ in the interval $[\omega_A, \omega_B]$. Taylor series expansion is used for approximating $(\frac{1+\frac{s}{\omega_B}}{1+\frac{s}{\omega_A}})^n$ and truncated so as to obtain a second-order transfer function for $C_{(n)}$. Moreover, it is also proved that both approximations are stable when the fractional differentiation order n is: $0 < n < 1$. This is not restrictive because when $\{n\} > 1$, only fractional part of the differentiation or integration is approximated. Consequently, (22) and (23) can be used to approximate any fractional differentiator or integrator.

Step 2 – Approximation of $s^{-n}_{[\omega_A,\omega_B]}$ by continuous-time rational models

The irrational fractional part of $s^{-n}_{[\omega_A,\omega_B]}$ can be approximated by a Taylor series expansion, a continuous fraction expansion, or a recursive distribution of poles and zeros. In all cases a truncation is necessary to be able to simulate the obtained model. The greater the truncation order, the better the approximation.

i) Series expansions

The last element of (19), (20), (22), and (23) is now written using $u(s)$:

$$\left(\frac{1+\frac{s}{\omega_B}}{1+\frac{s}{\omega_A}}\right)^n = (1+u(s))^n \tag{24}$$

where

$$u(s) = \frac{-s/\omega_A + s/\omega_B}{1+s/\omega_A}$$

$|u(s)| < 1$ within the frequency range $]\omega_A, \omega_B]$. Hence, the series expansion is convergent. (24) can be approximated by truncating (25) and (26):

Taylor Series expansion

$$(1+u(s))^n = \sum_{i=0}^{\infty}\left(\binom{i}{n}(u(s))^i\right) \tag{25}$$

Continuous fraction expansion

$$(1+u(s))^n = 1 + \frac{u(s)}{a_1 + \frac{u(s)}{a_2 + \frac{u(s)}{a_3+\cdots}}} \tag{26}$$

ii) Approximation with recursive poles and zeros [20, 24]

$$s^{-n}_{[\omega_A,\omega_B]} \cong \left(\frac{1}{\omega_A}\right)^n \prod_{k=-N}^{N}\left(\frac{1+\frac{s}{\omega_k}}{1+\frac{s}{\omega'_k}}\right) \tag{27}$$

where ω_k and ω'_k are respectively zeros and poles of rank k. They are recursively distributed in the desired frequency range.

$$\alpha = \omega_k/\omega'_k \quad \text{and} \quad \eta = \omega'_{k+1}/\omega'_k \tag{28}$$

Table 2. Asymptotic behavior of the four models.

Asymptotic behavior of model	(19)	(20)	(22)	(23)
Phase (deg)				
Low frequency	0	−90	0	−90
High frequency	0	−90	−90	0
Magnitude (dB)				
Low frequency	Finite	∞	Finite	∞
High frequency	Finite	∞	∞	finite

α and η satisfy:

$$n = \log(\alpha/\eta)/\log(\alpha\eta) \tag{29}$$

Approximations (19), (20), (22), and (23) are compared in Figures 2 and 3. It can be seen that the performance of approximations (19) and (20) depends on the differentiation order n. (19) gives better results than (20) for differentiation orders $0 < n < 0.5$ and (20) gives better results than (19) for differentiation orders $0.5 < n < 1$.

The improved methods make the approximations completely independent of the differentiation order. In addition, the approximation procedure does not depend on an arbitrary choice of tuning parameters. The synthesis is carried out knowing high and low frequencies (Table 2).

For instance, the improvements in the boundary effects are visible in Figure 2 for a differentiation order of 0.2. Although the phase is the same at around 10^{-3} rad/s, the new approximation is nearer to the true value around $\omega_A = 10^{-2}$ rad/s and $\omega_B = 10^2$ rad/s.

Step 3 – Approximation of the fractional model output

Various algorithms have been developed for computing a model's output on the basis of the transfer function or state–space representation. Starting from a fractional transfer function, a rational model is obtained by substituting each fractional differentiation operator in (10) by a band-limited approximation as synthesized in Step 2. The model output is then the convolution of the integer model with the input signal.

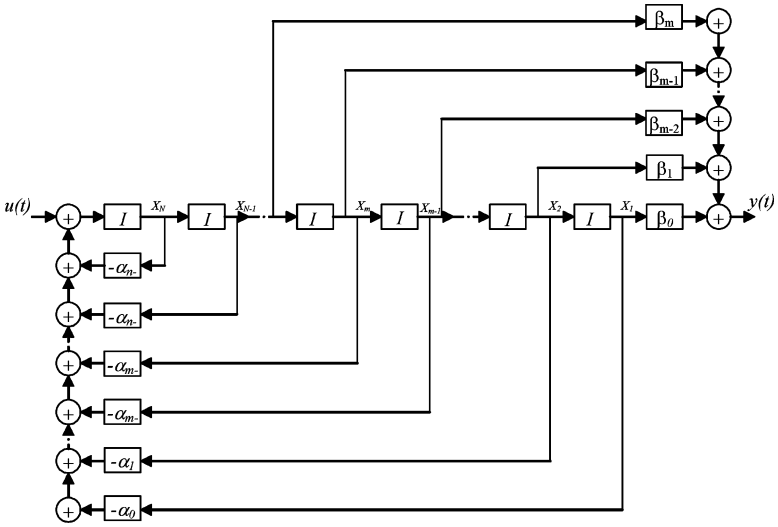

Figure 4. Series simulation schema.

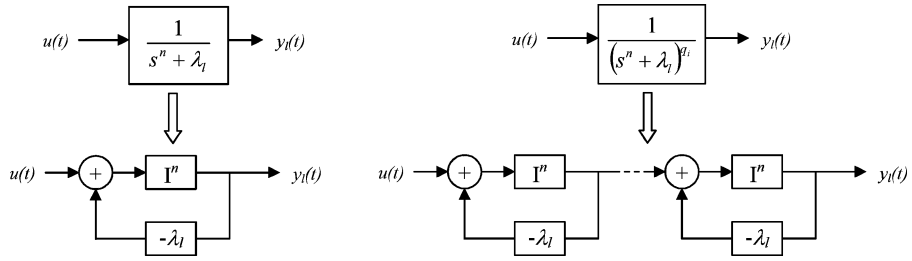

Figure 5. Simulation schema of one eigenmode. (left: simple eigenmode, right: multiple eigenmode).

By using a companion state–space representation, Lin proposes a series configuration of the integer model as shown in Figure 4 [20]. The drawback of such a simulation method is that the error multiplies rapidly due to the series nature of the model.

A new method is now proposed. It is based on modal representation (11). As the output of the model is a linear combination of eigenmodes, each eigenmode contribution can be simulated separately. The output of one simple eigenmode is represented as shown in Figure 5. I^n represents the fractional integrator approximation in a limited frequency band as described by (19), (20), (22) and (23).

As the output model is a linear combination of eigenmode outputs, the computational time is short and the approximation error is smaller compared to methods that use a series configuration. From a digital implementation point of view, the numerical stability of this schema is very useful and moreover computations can be parallelized.

4. Numerical Examples

4.1. Example 1

The objective is to compute the step response of:

$$H_1(s) = \frac{1}{s^{0.25}} \tag{30}$$

Integrator (30) was chosen because its response is known analytically (15). Hence, various approximations can be compared to the true response:

$$y_1(t) = \frac{1}{\Gamma(1.25)} t^{0.25}. \tag{31}$$

The step response will be approximated using a rational continuous-time model equivalent to H_1 in the frequency range [0.01, 100].

In Figure 7, the step response was plotted for all the four approximations (19), (20), (22) and (23). It is evident that the output obtained by (20) fails to approximate the known analytical response correctly because the fractional order 0.25 is small compared to 1. On the other hand, if the integration order was chosen to be 0.75 instead of 0.25, approximation (19) would have failed to capture the dynamics because 0.75 is great compared to 0. However, both approximations (22) and (23) perform better whatever the differentiation order. Note that the obtained approximation is valid only within the frequency range [0.01, 100].

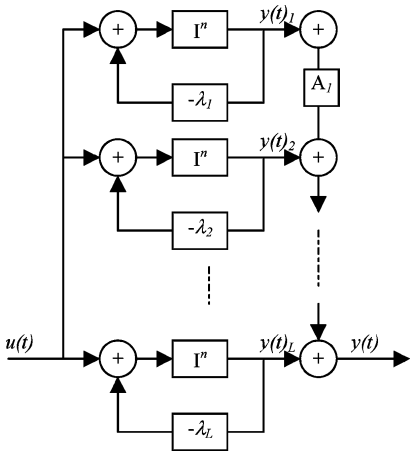

Figure 6. Simulation schema of a fractional system having only simple eignemodes.

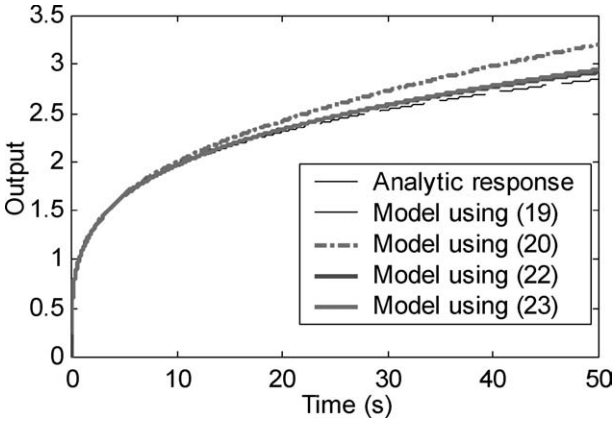

Figure 7. Step response of fractional integration with order 0.25. Response of models (20) and (23) and the analytic one are almost superposed.

4.2. Example 2

Consider a fractional continuous-time system:

$$H_2 = \frac{0.1}{s^{0.8}+1} + \frac{1}{s^{0.8}+10} \tag{32}$$

The analytic step response of H_2 can be achieved using (14) and (17). Its expression is not easy to obtain and must be computed numerically. Since, the step response depends on the precision used when computing the convolution product in (14) and the integral in (17), it is simulated using an integer equivalent model. The fractional behavior is limited to the frequency band [0.01, 100] using models (19), (20), (22) and (23). The band-limited fractional integration is approximated using eight poles. The simulation result is shown in Figure 9. The three approximations (20), (22), and (23) exhibit equivalently good results. However, approximation (19) now shows poor results because the commensurate order is close to 1.

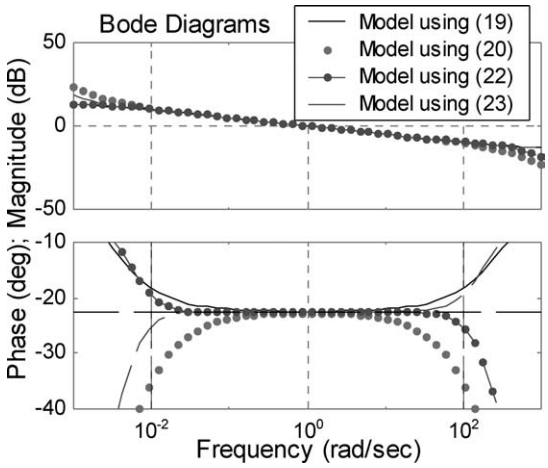

Figure 8. Bode diagram of a fractional integration of order 0.25 approximated with (19), (20), (22) and (23) within the frequency range [0.01, 100]. Model (20) is not satisfactory as the order n is close to 0.

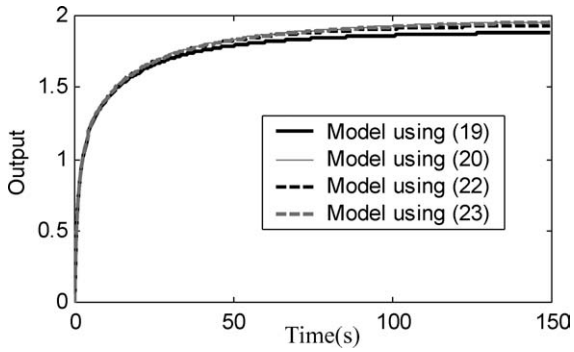

Figure 9. Step response of H_2 using equivalent integer continuous model in the frequency range [0.01, 100]. Approximations (20), (22) and (23) are almost indistiguishable.

5. Conclusion

An overview of existing simulation methods of fractional systems has been given, and improvements proposed for approximating fractional models by continuous-time rational models. The aim is two-fold: the reduction of approximation error close to the extremities of the frequency band, also the decrease of system output sensitivity to differentiation orders. No adjustment coefficients are needed in the proposed method. To achieve satisfactory approximation only frequency bandwidth is needed.

Appendix

SYNTHESIS OF (22)

Let the fractional transfer function be

$$K(s) = \left(\frac{1 + \frac{s}{\omega_B}}{1 + \frac{s}{\omega_A}} \right)^n, \quad 0 < n < 1,\ s = jw. \tag{33}$$

Thus

$$K(s) = \left(\frac{\omega_A}{s}\right)^n \left(1 + \frac{s^2 - \omega_A\omega_B}{\omega_A\omega_B + s\omega_B}\right)^n. \tag{34}$$

As

$$\left|\frac{s^2 - \omega_A\omega_B}{\omega_A\omega_B + s\omega_B}\right| < 1, \quad \forall\omega_A < \omega < \omega_B, \tag{35}$$

using a Taylor series expansion

$$K(s) = \left(\frac{\omega_A}{s}\right)^n \left(1 + nu(s) + \frac{n*(n-1)}{2}u^2(s) + \cdots\right) \tag{36}$$

with

$$u(s) = \frac{s^2 - \omega_A\omega_B}{\omega_A\omega_B + s\omega_B}.$$

Combining (33) and (33) yields:

$$\left(\frac{1}{s}\right)^n = \frac{(\omega_A)^{-n}}{\left(1 + nu(s) + \frac{n*(n-1)}{2}u^2(s) + \cdots\right)} \left(\frac{1 + \frac{s}{\omega_B}}{1 + \frac{s}{\omega_A}}\right)^n \tag{37}$$

Truncating the Taylor series to 1 term leads to

$$\left(\frac{1}{s}\right)^n \cong \frac{1}{(\omega_A)^n(1 + nu(s))} \left(\frac{1 + \frac{s}{\omega_B}}{1 + \frac{s}{\omega_A}}\right)^n \tag{38}$$

Thus

$$\left(\frac{1}{s}\right)^n \cong \frac{\omega_A\omega_B + s\omega_B}{(\omega_A)^n(ns^2 + s\omega_B + (1-n)\omega_A\omega_B)} \left(\frac{1 + \frac{s}{\omega_B}}{1 + \frac{s}{\omega_A}}\right)^n \tag{39}$$

Relation (39) approximates a fractional integration of order n if $0 < n < 1$.

STABILITY OF (22), OR (39)

Expression (39) is stable if all the poles are on the left-hand side of the complex s-plane. It is easy to check that (39) has three poles:

- one pole: root of $\left(1 + \frac{s}{\omega_A}\right)$ which is negative because $\omega_A > 0$;
- and two poles: roots of $(ns^2 + s\omega_B + (1-n)\omega_A\omega_B)$ whose real parts are negative when $n > 0$, $\omega_B > 0$ and $(1-n)\omega_A\omega_B > 0$ (the last condition is satisfied when $n < 1$).

Thus all poles of (39) are stable provided $0 < n < 1$.

Hence, (39) is a stable approximation a fractional integrator of order n ($0 < n < 1$) within the frequency range $[\omega_A, \omega_B]$.

SYNTHESIS OF (23)

As above, start by defining $K(s)$:

$$K(s) = \left(\frac{1 + \frac{s}{\omega_{\mathrm{A}}}}{1 + \frac{s}{\omega_{\mathrm{B}}}} \right)^{n-1} \tag{40}$$

Then, using a Taylor series expansion:

$$K(s) = \left(\frac{1}{s} \right)^{n} s\omega_A^{n-1}(1 + (1-n)u(s) + \cdots)^{-1} \tag{41}$$

with

$$u(s) = \frac{s^2 - \omega_{\mathrm{A}}\omega_{\mathrm{B}}}{\omega_{\mathrm{A}}\omega_{\mathrm{B}} + s\omega_{\mathrm{B}}}.$$

Substituting $K(s)$ and $u(s)$ and then truncating Taylor series expansion to 1 term, yields approximation (23) of the fractional integral in $[\omega_{\mathrm{A}}, \omega_{\mathrm{B}}]$:

$$\left(\frac{1}{s} \right)^{n} \cong \frac{\omega_{\mathrm{A}}^{1-n}}{s} \left(\frac{(1-n)s^2 + \omega_{\mathrm{B}}s + n\omega_{\mathrm{A}}\omega_{\mathrm{B}}}{\omega_{\mathrm{A}}\omega_{\mathrm{B}} + s\omega_{\mathrm{B}}} \right) \left(\frac{1 + \frac{s}{\omega_{\mathrm{B}}}}{1 + \frac{s}{\omega_{\mathrm{A}}}} \right)^{n-1}.$$

The aim of this approximation is to achieve an asymptotic behavior corresponding to an integrator at low frequencies. Hence, there is a pole at 0. The other poles are stable as they are located at: $-\omega_A$ and $-\omega_B$.

References

1. Ichise, M., Nagayanagi, Y., and Kojima, T., 'An analog simulation of non integer order transfer functions for analysis of electrode processes', *Journal of Electroanalytical Chemistry Interfacial Electrochemistry* **33**, 1971, 253.
2. Darling, R. and Newman J., 'On the short behavior of porous intercalation electrodes', *Journal of Electrochemical Society* **144**(9), 1997, 3057–3063.
3. Battaglia, J. L., Cois, O., Puigsegur, L., and Oustaloup, A., 'Solving an inverse heat conduction problem using a non-integer identified model', *International Journal of Heat and Mass Transfer* **44**(14), 2001, 2671–2680.
4. Cois, O., 'Systèmes linéaires non entiers et identification par modèle non entier: application en thermique', Ph.D. Thesis, University of Bordeaux I, France, 2003.
5. Bode, H. W., *Network Analysis and Feedback Amplifiers Design*, Nostrand, New York, 1945.
6. Tustin, A., Allanson, J. T., Layton, J. M., and Jakeways, R. J., 'The design of systems for automatic control of the position of massive object', in *Proceedings of Institution of Electrical Engineers*, 1958, 105, Part C, Suppl. 1, pp. 1–57.
7. Oustaloup, A., Systèmes asservis linéaires d'ordre fractionnaire, Masson, Paris, 1983.
8. Al-Alaoui, M. A., 'Novel IIR differentiator from the Simpson Integration rule', *IEEE Transactions on Circuits and Systems I. Fundamental Theory and Applications* **41**(2), 1994, 186–187.
9. Vinagre, B. M., Podlubny, I., Hernandez, A., and Feliu, V., 'Some approximations of fractional order operators used in control theory and applications', *Fractional Calculus & Applied Analysis* **3**(3), 2000, pp. 231–248.
10. Petras, I., Podlubny, I., O'Leary, P., and Dorcak, L., 'Analogue fractional-order controllers: Realization, tuning and implementation', in *Proceedings of the ICCC'2001*, Krynica, Poland, 2001, pp. 9–14.
11. Chen, Y. Q. and Kevin, L. Moore, L., 'Discretization schemes for fractional-order differentiators and integrators', *IEEE Transactions on Circuits and Systems-I: Fundamental Theory and Applications* **49**(3), 2002, 363–367.

12. Chen, Y. Q., Vinagre, B., and Podlubny, I., 'A new discretization method for fractional order differentiators via continued fraction expansion', in *ASME First Symposium on Fractional Derivatives and Their Applications*, *International Design Engineering Technical Conferences*, Chicago, Illinois, 2003.
13. Podlubny, I., *Fractional Differential Equations*. Mathematics in Science and Engineering, Vol. III. Academic Press, San Diego, California, 1999.
14. Podlubny, I., Petras, I., Vinagre, B. M., O'Leary, P., and Dorcak, L., 'Analogue realizations of fractional-order controllers', *Nonlinear Dynamics* **29**(1–4), 2002, 281–296.
15. Petras, I., Podlubny, I., O'Leary, P., Dorcak, L., and Vinagre, B., *Analogue Realization of Fractional Order Controllers*, Technical University of Kosice, Kosice, Slovak Republic, 2002, p. 84.
16. Samko, S. G., Kilbas, A. A., and Marichev, O. I., *Fractional Integrals and Derivatives: Theory and Applications*. Gordon and Breach, Amsterdam, 1993.
17. Miller, K.S. and Ross, B., *An Introduction to the Fractional Calculus and Fractional Differential Equations*. Wiley, New York, 1993.
18. Oldham, K. B. and Spanier, J., *The Fractional Calculus*. Academic Press, New York, 1974.
19. Matignon D., 'Représentations en variables d'état de modèles de guides d'ondes avec dérivation fractionnaire', Ph.D. Thesis, Université de Paris-Sud, Orsay, France, 1994.
20. Oustaloup, A., La dérivation non Entière: Théorie, Synthèse et Applications, Hermès, Paris, 1995.
21. Matignon, D., 'Stability properties for generalized fractional differential systems', in *ESAIM: Proceedings, Vol. 5, Systèmes Différentiels Fractionnaires – Modèles, Méthodes et Applications,* Paris, 1998.
22. Tabak, D., 'Digitalization of control systems', *Computer Aided Design* **32**, 1971, 13–18.
23. Lin, J., 'Modélisation et identification de systèmes d'ordre non entier', Thèse de Doctorat, Université de Poitiers, France, 2001.
24. Oustaloup, A., Levron, F., Nanot, F., and Mathieu, B., 'Frequency-band complex non integer differentiator: Characterization and synthesis', *IEEE Transaction on Circuits and Systems* **47**(1), 2000.